

File

I.O.S.

**ON THE MEASUREMENT OF NEAR SURFACE CURRENTS,
INCLUDING THE CONTRIBUTION FROM STOKES DRIFT**

R.M. CARSON and P.G. COLLAR

IOS REPORT NO 40

1977

**NATURAL ENVIRONMENT
INSTITUTE OF OCEANOGRAPHIC
SCIENCES
RESEARCH COUNCIL**

INSTITUTE OF OCEANOGRAPHIC SCIENCES

**Wormley, Godalming,
Surrey, GU8 5UB.
(0428 - 79 - 4141)**

(Director: Professor H. Charnock)

**Bidston Observatory,
Birkenhead,
Merseyside, L43 7RA.
(051-653-8633)**

(Assistant Director: Dr. D. E. Cartwright)

**Crossway,
Taunton,
Somerset, TA1 2DW.
(0823-86211)**

(Assistant Director: M. J. Tucker)

**Marine Scientific Equipment Service
Research Vessel Base,
No. 1 Dock.
Barry,
South Glamorgan, CF6 6UZ.
(0446-737451)
(Officer-in-Charge: Dr. L. M. Skinner)**

*On citing this report in a bibliography the reference should be followed by
the words UNPUBLISHED MANUSCRIPT.*

ON THE MEASUREMENT OF NEAR SURFACE CURRENTS,
INCLUDING THE CONTRIBUTION FROM STOKES DRIFT

R.M. CARSON and P.G. COLLAR

IOS REPORT No. 40

1977

INSTITUTE OF OCEANOGRAPHIC SCIENCES
WORMLEY, GODALMING, SURREY, ENGLAND

Introduction

This report is concerned with the problem of measuring near-surface current in the presence of waves. Our main thesis is that it should be possible to measure surface current from a loosely-moored surface-following buoy, and that this measurement will include the Stokes Drift due to locally generated waves; it will thus give a result which is comparable to that of a fully-Lagrangian drifter at the same point. This measurement is no less useful than that of a fixed-point current meter, which measures current without Stokes Drift; and it is a system which may be more easily realised in the open sea than a truly fixed point measurement.

The importance of Stokes Drift has been demonstrated by Kenyon (1969, 1970) who calculated the expected magnitude in different sea states and found it to be a significant fraction of the Ekman wind-driven current. Ursell (1950) showed that the Stokes Drift must vanish on a rotating earth (see also Hasselmann, 1970 and Pollard 1970); but Ianniello and Garvine (1975) have demonstrated that locally-generated Stokes Drift will still be a significant effect in commonly-occurring oceanic conditions of duration and fetch-limited waves.

Theory

Using classical small-amplitude wave theory, we have calculated the expected output from a near-surface current meter constrained to move in a variety of geometries. The results are summarised in Table 1; the detailed analysis is in the Appendices. The conclusions are:

- (1) A fixed point current meter does not measure the Stokes Drift

$$S = a^2 \tau k e^{-2kz_0} \quad (\text{for symbols see Definition List})$$

- (2) A current meter which is constrained to follow a closed circular path, which as nearly as possible overlays the actual path of the water particle, and whose axis is maintained horizontal, measures the Stokes Drift exactly.
- (3) If the circular path is relaxed to allow the buoy its natural non-circular motion, the Stokes Drift is still measured correctly, to 1st order in ak .
- (4) If the constraint is further relaxed, so that the buoy/current meter follows the water surface and the current meter axis is tangential to the wave slope, we still measure Stokes Drift to 1st order ak ; but we do so for a different reason.
(Compare \bar{V}_{cm} , \bar{V}_p for the two geometries.)
- (5) If we extend the current meter stem below the buoy, to a depth h , we incur an error in measuring Stokes Drift at that depth. However this is such that the measurement can be related, to first order, to the Stokes Drift at the level of the buoy.
- (6) The finite buoy diameter is responsible for a high-frequency cut-off in shorter waves: this is significant for wavelengths of less than three buoy diameters; for a buoy of 2m diameter or less, the effect on measured current will be negligible in a typical sea.

We have assumed in these calculations that we possess:

- (a) a perfect current meter, which is linear, and measures the component of velocity along a chosen axis irrespective of the actual flow vector direction. (i.e. no hydrodynamic stalling.)
- (b) a perfect mooring which is compliant with respect to wave amplitudes and periods, but which restrains the buoy from drifting over the measuring period.

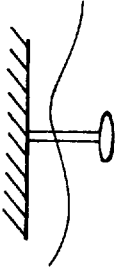
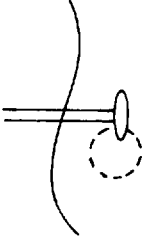




Geometry	Integrated velocity of current meter along axis \bar{V}_{cm}	Integrated particle velocity along axis \bar{V}_p	Integrated current meter output $\bar{V}_p - \bar{V}_{cm}$	Degree of approximation
1.  Fixed point axis horizontal	0	0	0	Exactly
2.  Best-fit circular path. Axis horizontal	0	$a^2 \sigma k e^{-2kz} \circ$	$a^2 \sigma k e^{-2kz} \circ$	Exactly (cf. Pollard 1973)
3.  Non-circular path, true surface follower: axis horizontal, short stem	0	$a^2 \sigma k e^{-2kz} \circ$	$a^2 \sigma k e^{-2kz} \circ$	To 1st order in ak

TABLE 1 (continued)

SUMMARY OF RESULTS	TABLE 1 (continued)	Degree of approximation
Geometry	Integrated velocity of current meter along axis \bar{V}_{cm}	Integrated particle velocity along axis \bar{V}_p
Integrated velocity of current meter along axis \bar{V}_{cm}	Integrated current meter output $\bar{V}_p - \bar{V}_{cm}$	
<p>4.</p>  <p>Circular path, short stem, axis parallel to surface/streamline</p>	$-\frac{1}{2} a^2 \sigma k e^{-2kz} \circ$	$\frac{1}{2} a^2 \sigma k e^{-2kz} \circ$
<p>5.</p>  <p>Surface follower, long stem h, axis parallel to surface</p>	$-\frac{1}{2} a^2 \sigma k e^{-2kz} \circ$	$\frac{1}{2} a^2 \sigma k e^{-2kz} \circ$ $X e^{-kh} (1 + hk)$ $\sim \frac{1}{2} a^2 \sigma k e^{-2kz} \circ$
<p>6.</p>  <p>Lagrangian Drifter</p>	$a^2 \sigma k e^{-2kz} \circ$	<p>Exactly</p>

It must be emphasised that in the tank we are dealing with orbital velocities $\sim 10\text{cm/sec}$ and drift velocities $\sim 1\text{cm/sec}$ and difficulties of calibration and especially of zero accuracy of the current meter are considerable. We found that drift currents persisted in the tank for several hours and that strong shears were generated. Thus to obtain an accurate zero reading, it was essential to use dye to check the actual flow at the current meter head; a significant flow frequently existed at say 10cm depth, when the surface current had reached negligible values. In making the dye/current meter observation, it was equally important to use dye at the correct mean depth, and to average the result over 5-10 wave cycles, as there was some variation from wave to wave. We also found it necessary to synchronise the current meter record with film of the dye motion, so that the same waves were used for the comparison.

Some of these precautions we learned by experience, and where large error bars occur on the results, this indicates an early run where the zero calibration is not accurately known.

Results

These are shown as scatter diagrams in Fig.1(a)-(e), in which current has been varied using a range of wave heights and periods (0-25cm, 1.0-2.2s). The main results can be summarized as:

- (a) The fixed spar current meter (x,z) does indeed fail to measure the contemporary Stokes Drift; the actual measured drift is in the reverse direction. By turning the current meter through 10° or 30° , to the direction of wave propagation, we obtained a result which agrees better with the dye observations. This agreement is spurious, being solely due to the stalling behaviour of the current meter head during part of the wave cycle.
- (b) The fixed spar current meter (x,y) stalls during a large part of the wave cycle, giving a false answer.
- (c) The surface following buoy, restrained in pitch and surge, is an unsatisfactory compromise (cf. Pollard, 1973 analysis).

- (d) The discus buoy is moderately satisfactory if the current meter stem is intermediate in length (9cm). A very long stem introduces errors due to buoy pitching. A very short stem brings the head into a trapped boundary region, about 5cm thick, where the net flow bears no relation to the drift outside. Stalling is not a problem, because flow is generally parallel to the sensor plane.
- (e) The surface following catamaran allows the sensor to be brought very close to a free water surface, while avoiding the boundary region problem. Again, a long stem could introduce buoy pitching errors.

Discussion

The results generally bear out the theoretical expectations. In particular the fixed spar (a) and the catamaran (e) demonstrate very clearly the difference between the fixed point Eulerian measurement and the pseudo-Lagrangian buoy measurement. The most important practical conclusion of the tests, however, is the observation that a flat discus buoy traps a surprisingly thick boundary region beneath it. The mechanism appears to be that the buoy, in pitching over the wave crest, captures a volume of water beneath it at the moment when this water might be expected to move on, out from beneath the buoy. This region is thicker than the boundary layer which would form due to a steady drift shear flow. This is an important consideration in the design of any practical system.

Measurements at sea

We now attempted to realise a sea going system in which the sea surface immediately above the current meter was undisturbed to avoid any boundary layer. The obvious system to use, particularly in view of a shortage of time, was the IOS pitch/roll buoy (Clayson and Smith 1970), which could easily accommodate two additional channels for e.m. current meter output. Since this is usually coupled to the ship by an umbilical buoyant cable

carrying signals and power, the need for in situ vector averaging of current meter outputs was eliminated. We were not sure that the boundary layer would not be present in the present form of the buoy, however, and therefore adopted the modified arrangement shown in Fig.2. This EMPR buoy is maintained at a depth of 0.5m by three inflated floats. It is coupled to the attendant ship by the usual buoyant wave-buoy cable; this coupling was made compliant by forming a series of catenary loops, as shown in Fig.3.

Instrumentation

The x and y outputs of the current meter, together with the compass output and the heave data from the gyro-stabilised accelerometer were sampled at 0.5sec intervals and recorded in binary form on magnetic tape for subsequent analysis. Each run was continued for 20 minutes, and a simultaneous wave record was made using the Shipborne Wave Recorder fitted to the ship. The ship's e.m. log was also sampled and 2-minute averages were stored by the shipboard computing system.

Deployment

The buoy was launched from the foredeck of R.R.S. DISCOVERY, and paid out on the starboard bow of the ship. The ship was then held stationary relative to the buoy by the use of bow thruster and propeller; in general the windage of the ship results in the ship towing the buoy gently to windward. When the system seemed stable, a trawl float pinger, suspended 0.5m below an 8cm diameter float, was released from the ship's bow; this was allowed to float out freely, parallel to the EMPR cable until it was abaft of the buoy; it was then recovered using a 2mm nylon line attached to the pinger (this line was paid out slack during the pinger run). A single current vector was established by timing this pinger run, and is used for comparison with the EMPR buoy output integrated over the same period.

Run No.	<u>EMPR buoy</u>		<u>Ship's log</u>		<u>Pinger</u>	
	Mag cm/s	Direction	Mag cm/s	Direction	Mag cm/s	Direction
2	24	259°	13	261°	22	195°
3	18	82°	29	22°	40	87°
4	29	86°	30	125°	37	140°

Table 2 AVERAGE VALUES OVER THE PERIODS OF THE PINGER RUN, DERIVED FROM FIGS. 4(a)-(c)

Results

Four runs were made: the first was marred by instrument noise, and the fourth was run in almost calm conditions. We have plotted the vector-averaged results of Runs 2-4 as 'stick charts' where each 2 minute velocity vector is plotted from a new origin on the time axis. (Figs.4(a)-(c)). In Table 2 we show the averages made over the period of the pinger run.

In none of the three useful runs is the agreement between EMPR buoy, pinger and ship's e.m. log good. This is true even for the last series of measurements, made in very calm conditions, in which best agreement might have been expected.

We believe there are several reasons for this:

1. Problems of ship handling, and consequent use of propeller and bow thruster, were causing large variations in the magnitude and direction of flow in the measurement area. Note, for example, the large variations in relative ship position, evident from the ship's e.m. log vectors in Run 3.
2. The uncertainties in estimating pinger velocity and direction were fairly large. It had been hoped originally that drift velocity could be estimated fairly accurately from the Doppler shift of the signal received at the ship, and displayed on the echo-sounder Mufax. The free running oscillator in the pinger proved insufficiently stable for Runs 2 and 3, however, and we had to resort to rather crude visual estimates ($\pm 20\%$ in magnitude, $\pm 20^\circ$ in direction). The magnitude estimate for Run 4 was considerably better ($\pm 5\%$) because a crystal controlled oscillator had been fitted by this time and the Doppler shift method could be used.
3. The dynamics of the EMPR buoy were manifestly not as good as we had hoped. Considerable improvement should result from:
 - (a) increasing the surface float spacing
 - (b) using a rigid framework in place of the present system of ropes.

4. It is worth stressing that the discrepancies shown in Fig.4 are actually larger than the expected Stokes Drift component. Thus for Run 2 the Stokes Drift at 0.5m depth is 4.3cm/sec, calculated from the measured unidirectional wave spectrum; while the discrepancy in measured velocity is typically of order 10cm/sec.

Conclusions

We reiterate our belief that measurement of surface current is best made from a surface following buoy since in this way the contribution from the Stokes component is included with least uncertainty. Some care is required however, if boundary layer effects are to be avoided underneath a surface follower in very weak currents. Surface current measurements using a surface following buoy deployed from a ship will always risk contamination by the perturbation of flow around the ship's hull. A permanent long term mooring is the next logical development, although we must then face the problem of either reducing the wave and current data in situ, or of telemetering it for subsequent computer processing.

There is a limit to the depth at which useful measurements can be made from a surface follower, but the principle of including the Stokes component applies perfectly well at any depth subjected to wave action. As yet we have not devised a practical solution.

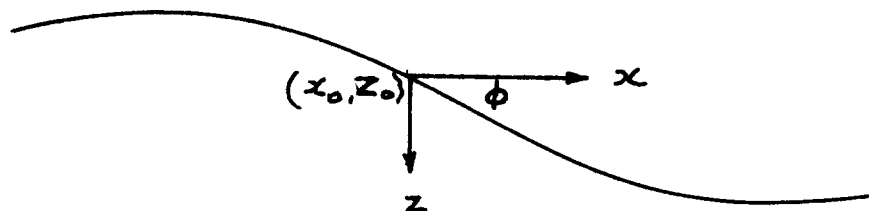
Acknowledgements

We are happy to acknowledge the assistance we have received from C.H. Clayson, V.A. Lawford, A.J. Bunting, G. Griffiths and J.A. Ewing.

References

- CLAYSON C.H. and SMITH N.D. (1970) Recent advances in wave buoy techniques at the National Institute of Oceanography, pp.289-306 in 'Electronic Engineering in Ocean Technology'. IERE.
- HASSELMANN K. (1970) Wave driven inertial oscillations. Geophys. Fluid Dyn. 1, 463-502.
- IANNIELLO J.P. and GARVINE R.W. (1975) Stokes Transport by gravity waves for application to circulation models. J. Phys. Ocean. 5, 47-50.
- KENYON K.E. (1969) Stokes Drift for random gravity waves. J. Geoph. Res. 74, 28, 6991-6994.
- KENYON K.E. (1970) Stokes Transport. J. Geoph. Res. 75, 6, 1133-1135.
- POLLARD R.T. 1970 Surface waves with rotation: an exact solution. J. Geoph. Res. 75, 30, 5895-8.
- POLLARD R.T. 1973 Interpretation of near-surface current meter observations. Deep-Sea Res. 20, 261-268.
- URSELL F. (1950) On the theoretical form of ocean swell on a rotating earth. Mon. Not. Roy. Astron. Soc. Geophys. Supp. 6, 1-8.

APPENDIX 1: Surface current measurement from a streamline follower



Defining axes as shown,

We assume a wave profile $\eta = a \sin(kx - \sigma t)$... (1)

The vertical and horizontal velocity components are:

$$V_z = a\sigma \cos(kx - \sigma t) \cdot e^{-kz} \quad \dots (2)$$

$$V_x = a\sigma \sin(kx - \sigma t) \cdot e^{-kz} \quad \dots (3)$$

(a) Current meter following streamline

If the mean position of the current meter is (x_0, z_0) , then at time t its position is:

$$[x, y] (t) = [x_0 + x_e(t), z_0 + z_e(x, t)] \quad \dots (4)$$

The exact forms of $x_e(t)$, $z_e(x, t)$ are very difficult to predict since one requires a priori knowledge of the mooring characteristics: they must, however, yield a closed orbit. We therefore follow Pollard (1973) and make $x_e(t)$ simple harmonic.

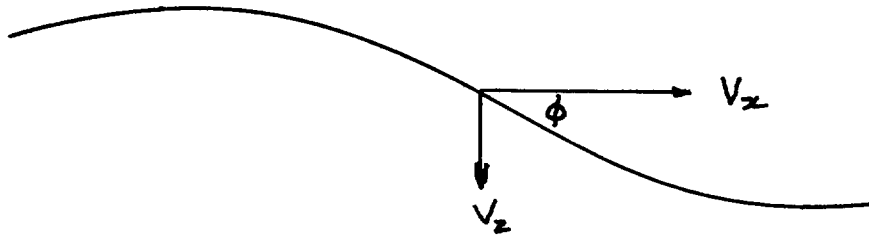
Then, for a surface following current meter,

$$[x, z] (t) = \left[x_0 + a \cos(kx_0 - \sigma t), z_0 - a \sin \left((kx_0 - \sigma t) + ak \cos(kx_0 - \sigma t) \right) \right] \\ \text{(in which } z_0 = 0) \quad \dots (5)$$

or, more generally, for a current meter following a streamline at a mean depth z_0 below the sea surface:

$$[x,z] (t) = \left[x_0 + a \cos(kx_0 - \sigma t) e^{-kz_0}, z_0 - a \sin \left((kx_0 - \sigma t) + ak \cos(kx_0 - \sigma t) \right) \cdot e^{-kz_0} \right] \dots (6)$$

We note from (6) that the current meter does not move in a circular path: the exact path is shown in Fig.5.



The local velocity at the current meter resolved tangentially to the streamline is $V_p = V_x \cos \phi + V_z \sin \phi$, while the current meter velocity resolved tangentially is $V_{cm} = V'_x \cos \phi + V'_z \sin \phi$. Therefore the flow measured by a current meter which follows a streamline, and whose axis is parallel to it, is:

$$V_{out} = V_p - V_{cm} = (V_x \cos \phi + V_z \sin \phi) - (V'_x \cos \phi + V'_z \sin \phi)$$

$$\text{where } \tan \phi \approx \phi \approx -\frac{\partial z}{\partial x} = -ak \cos(kx - \sigma t) \cdot e^{-kz_0} \text{ from (1)}$$

$$\approx -ak \cos \left(kx_0 - \sigma t + ake^{-kz_0} \cos(kx_0 - \sigma t) \right) \cdot e^{-kz_0} \dots (8)$$

Dealing first with V_p and substituting from (2), (3), (6) and (8)

$$V_p = a\sigma e^{-kz_0} \cdot e^{ak \sin(\theta + ak \cos \theta) \exp(-kz_0)} \cdot \sin \left(\theta + ak \cos \theta \cdot e^{-kz_0} - ake^{-kz_0} \cdot \cos(\theta + ake^{-kz_0} \cos \theta) \right)$$

$$\text{where } \theta = kx_0 - \sigma t$$

Expanding the exponential as a series and ignoring terms of order $a^3 k^3$ and above,

$$V_p = a \tau e^{-kz_0} \left[\sin \theta + ak \sin^2 \theta e^{-kz_0} + a^2 k^2 e^{-kz_0} \sin \theta \cos^2 \theta + \frac{a^2 k^2}{2} \sin^3 \theta e^{-2kz_0} + \frac{a^2 k^2}{2} \sin 2\theta \cos \theta e^{-kz_0} \right]$$

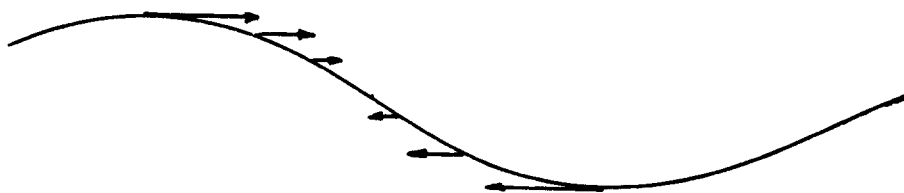
Integrating over a wave period, and dividing by 2π to obtain mean tangential flow at the current meter,

$$\bar{V}_p = \frac{a^2 \sigma k e^{-2kz_0}}{2} + \text{terms of order } a^2 k^2 \quad \dots (9)$$

which to order ak amounts to half the Stokes Drift component.

[We note that if the current meter were constrained to an exactly circular path \bar{V}_p would again be $\sim \frac{a^2 \sigma k e^{-2kz_0}}{2}$, but some differences would exist in higher order terms.]

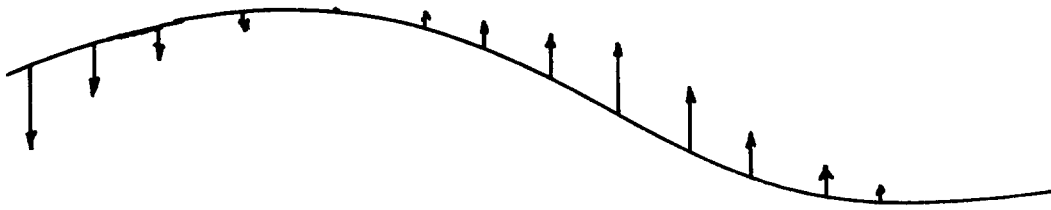
At first this result appears surprising, yet it arises because V_z , when resolved along the streamline, makes a net contribution to V_p . The effect is illustrated below



$$\int V_x = \bar{V}_{x \text{ hor}} = a^2 \sigma k e^{-2kz_0}$$

and

$$\int V_x \cos \phi \approx \bar{V}_{x \text{ hor}}$$

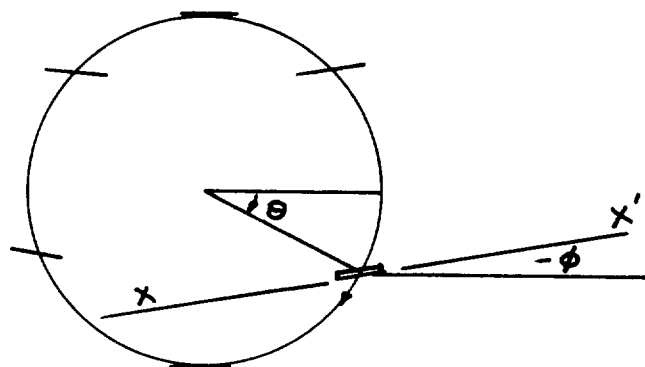


$$\int v_z = 0$$

but $\int v_z \sin \phi \approx -\frac{1}{2} a^2 \tau k e^{-2kz_0}$

hence $\int (v_x \cos \phi + v_z \sin \phi) = \bar{v}_p = \frac{a^2 \tau k e^{-2kz_0}}{2}$

Having found that the assumption of a circular path would involve only second order terms, we likewise make it in calculating the mean current meter velocity, resolved tangentially along the streamline, \bar{v}_{cm}



$xx' =$ current meter axis

Current meter path

$$V_{cm} = a \dot{\theta} e^{-kz_0} \cos \left(\frac{\pi}{2} - (\theta - \phi) \right)$$

$$\text{where } \phi \approx -ak \cos(\theta + ak e^{-kz_0} \cos \theta) e^{-kz_0}$$

Substituting for ϕ and integrating over a wave period,

$$\begin{aligned} \bar{V}_{cm} &= -e^{-kz_0} \frac{\sigma}{2\pi} \int_0^{2\pi/\sigma} a\tau(\sin\theta + ae^{-kz_0} \cos^2\theta) d\theta \text{ to first order in } ak \\ &= -\frac{a^2 \tau k e^{-2kz_0}}{2} \end{aligned} \quad \dots (10)$$

Since this velocity is in a direction opposite to that of wave propagation, we have, from (9) and (10)

$$\begin{aligned} \bar{V}_p - \bar{V}_{cm} &= \frac{a^2 \tau k e^{-2kz_0}}{2} - \left(-\frac{a^2 \tau k e^{-2kz_0}}{2} \right) \\ &= a^2 \tau k e^{-2kz_0} \end{aligned} \quad \dots (11)$$

which, to first order in ak , is the Stokes Drift component.

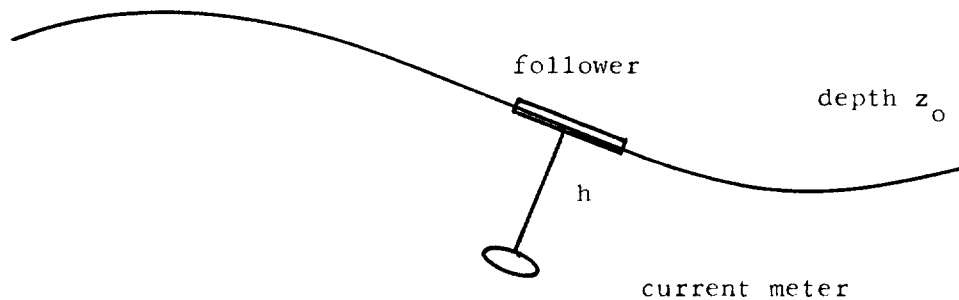
For a system which follows the streamline but measures only the horizontal component,

$$\bar{V}_p = a^2 \tau k e^{-2kz_0} \text{ exactly as remarked above}$$

and $\bar{V}_{cm} = 0$

Hence the Stokes Drift is measured exactly in this case.

(b) Current meter mounted at depth h below streamline follower



The expression (6) for the instantaneous position of the current meter now becomes:

$$\begin{aligned}
 [x, z](t) &= \left[\begin{array}{l} x_0 + ae^{-kz_0} \cos(kx_0 - \pi t) - h \sin \phi, \\ z_0 + h \sec \phi - ae^{-kz_0} \sin \left(kx_0 - \pi t + ake^{-kz_0} \cos(kx_0 - \pi t) \right) \end{array} \right] \\
 &\approx \left[\begin{array}{l} x_0 + a(1 + hk)e^{-kz_0} \cos(kx_0 - \pi t), \quad z_0 + h - ae^{-kz_0} \sin(kx_0 - \pi t) \end{array} \right] \\
 &\quad \text{for small } \phi \qquad \qquad \qquad \dots (12)
 \end{aligned}$$

The path thus approximates to an ellipse, centred on $(x_0, z_0 + h)$, of semi axes $a(1 + hk)e^{-kz_0}$, ae^{-kz_0}

As before, the flow along the current meter axis,

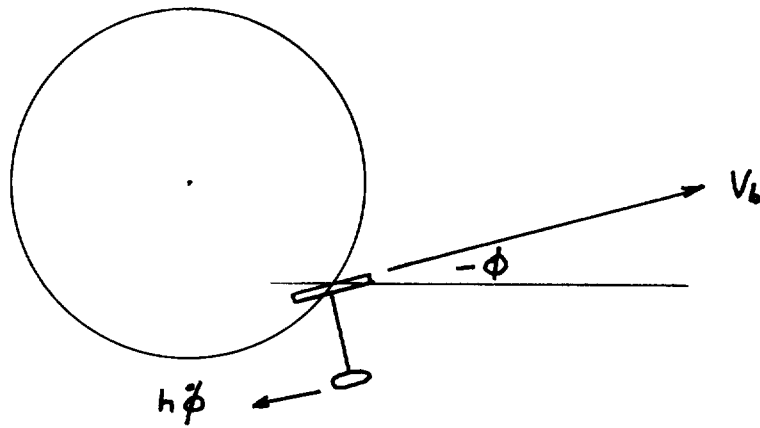
$$V_p = V_x \cos \phi + V_z \sin \phi$$

but where ϕ is now the wave slope at the follower rather than at the current meter.

From (2), (3), (8), (12), neglecting terms above $a^2 k^2$, we obtain an expression for V_p which on integration yields

$$\begin{aligned} \bar{V}_p &= \frac{a^2 \sigma k e^{-2kz_0}}{2} \cdot e^{-kh} \cdot (1 + hk) \quad \dots (13) \\ &\approx \frac{a^2 \sigma k e^{-2kz_0}}{2} \text{ for } hk \ll 1 \text{ as in (9)} \end{aligned}$$

The velocity at the current meter parallel to the streamline through the follower is now given by



$$V_{cm} = V_b - h\dot{\phi} \quad \text{where } V_b = \text{buoy velocity}$$

$$\therefore \bar{V}_{cm} = \bar{V}_b - \overline{h\dot{\phi}}$$

where \bar{V}_b is now given by equation (10). Equation (8) taken over a wave period yields $\overline{h\dot{\phi}} = 0$.

Hence the current meter measures

$$\begin{aligned} \overline{V_p - V_b} &= \frac{a^2 \sigma k e^{-2kz_0}}{2} \left(1 + (1 + hk)e^{-hk} \right) \quad \dots (14) \\ &\approx a^2 \sigma k e^{-2kz_0} \text{ which, again, is Stokes Drift at the depth} \end{aligned}$$

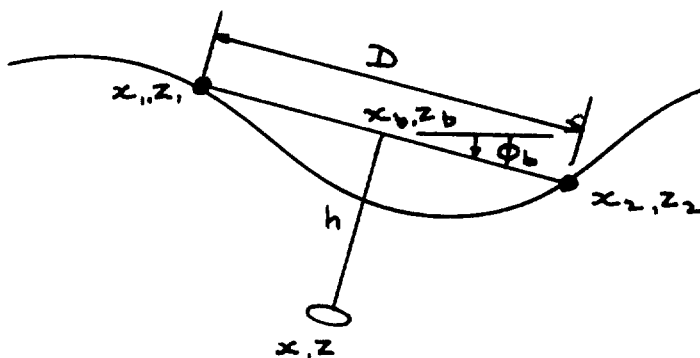
of the buoy.

Thus we are left with the very surprising but useful conclusion that, provided $kh \ll 1$, the errors incurred by mounting the current meter below the follower are such that the measurement can always be equated (to first order) to the Stokes Drift at the depth of the follower itself.

APPENDIX 2: Performance of a surface follower in short waves

The preceding analysis has assumed that the buoy is a perfect surface follower, i.e. the buoy pitch angle ϕ is always equal to the local streamline gradient. In any practical system there will always be waves present which are comparable in wavelength to the buoy diameter; these the buoy cannot follow, and we must estimate the effect which this has on the current meter output.

We avoid the detailed consideration of buoy dynamics by assuming a very simple model; two small floats, each taken to be a surface follower ($z_0 = 0$), are connected rigidly together on a spacing D which is comparable to the wavelength λ . The current meter is mounted a distance h below the floats.



If the wave profile is again $\eta = a \sin(kx - \sigma t)$ we may write the displacements z_1 and z_2 of the floats as

$$\left. \begin{aligned} z_1 &= -a \sin \left(kx_b - \frac{kD}{2} - \sigma t \right) \\ z_2 &= -a \sin \left(kx_b + \frac{kD}{2} - \sigma t \right) \end{aligned} \right\} \dots (15)$$

where x_b is the coordinate of the buoy mid-point.

Hitherto we have assumed that the displacement x of the buoy is simple harmonic, and deduced z , giving a non-circular orbit. We also found that the difference between a circular and non-circular orbit was second-order.

Here we do not make an assumption about the orbit; there is no a priori reason why it should be circular.

Rather, assume that \dot{x}_b , the buoy lateral velocity, is the mean of the fluid velocities acting on the small floats; this is equivalent to equating the drag forces on the floats while ignoring inertia and mooring forces.

$$\begin{aligned} \text{Then } \dot{x}_b &= \frac{1}{2} (Vx_2 + Vx_1) \\ &= \frac{1}{2} a\sigma \left[\sin(kx_b - \sigma t + \frac{kD}{2}) + \sin(kx_b - \sigma t - \frac{kD}{2}) \right] \dots (16) \end{aligned}$$

$$\begin{aligned} \text{But } z_b &= \frac{1}{2} (z_2 + z_1) \\ &= -\frac{1}{2} a \left[\sin(kx_b - \sigma t + \frac{kD}{2}) + \sin(kx_b - \sigma t - \frac{kD}{2}) \right] \dots (17) \end{aligned}$$

$$\text{so } \ddot{x}_b = -\sigma z_b$$

for which the solution is a circle.

Although we have shown that the orbit is a circle, we have not actually shown that the circumferential velocity is constant. However, to make further progress we must assume that it is, so that we may write

$$\begin{aligned} x_b &= x_o + a \cos(kx_o - \sigma t) \cos \frac{kD}{2} \\ \text{and } z_b &= -a \sin(kx_o - \sigma t) \cos \frac{kD}{2} \end{aligned} \quad \left. \vphantom{\begin{aligned} x_b \\ \text{and } z_b \end{aligned}} \right\} \dots (18)$$

We now re-write equation (12) with these modified values, as

$$[x, z](t) = \left[\begin{aligned} x_o + a \cos(kx_o - \sigma t) \cos \frac{kD}{2} - h \sin \phi_b, \\ z_o + h \sec \phi_b - a \sin(kx_o - \sigma t) \cos \frac{kD}{2} \end{aligned} \right] \dots (19)$$

where x, z refers to the current meter.

$$\text{Also } \sin \phi_b = \frac{z_2 - z_1}{D} = -\frac{2a}{D} \sin \frac{kD}{2} \cos(kx_o - \sigma t) \dots (20)$$

Using small angle approximation for ϕ_b and putting $kx_o - \sigma t = \theta$,
and $z_o = 0$,

$$\begin{aligned} (x, z) (t) &= \left(x_0 + a \cos \theta \cos \frac{kD}{2} + \frac{2ah}{D} \cos \theta \sin \frac{kD}{2}, \quad h - a \sin \theta \cos \frac{kD}{2} \right) \\ \phi_b &= - \frac{2a}{D} \cos \theta \sin \frac{kD}{2} \end{aligned} \quad \dots (21)$$

As before, $V_p = V_x \cos \phi_b + V_z \sin \phi_b$

whence $V_p = a \tau e^{-kh} \left(1 + ak \sin \theta \cos \frac{kD}{2} \right) \times$
 $\sin \left(\theta + ak \cos \theta \cos \frac{kD}{2} + \frac{2a}{D} (hk-1) \cos \theta \sin \frac{kD}{2} \right) \quad \dots (22)$

where we have ignored terms in $a^2 k^2$ and above.

$$\begin{aligned} V_{cm} &= a \dot{\theta} \sin(\theta - \phi_b) - h \dot{\phi}_b \quad \text{by analogy with equation 10} \\ &= - a \tau \left(\sin \theta + \frac{2a}{D} \cos^2 \theta \sin \frac{kD}{2} - \frac{2h}{D} \sin \theta \sin \frac{kD}{2} \right) \quad \dots (23) \end{aligned}$$

Integrating over a wave period to give mean values, we obtain:

$$\begin{aligned} \bar{V}_p &= \frac{a^2 \tau k e^{-kh}}{2} \left[2 \cos \frac{kD}{2} + (hk-1) \frac{\sin kD/2}{kD/2} \right] \\ \text{and } \bar{V}_{cm} &= - \frac{a^2 \tau}{D} \sin \frac{kD}{2} = - \frac{a^2 \tau k}{2} \frac{\sin kD/2}{kD/2} \end{aligned}$$

The measured current is therefore $\bar{V}_p - \bar{V}_{cm}$

$$= S \left[\cos \frac{kD}{2} e^{-kh} + \frac{\sin kD/2}{kD/2} \left(\left(\frac{hk-1}{2} \right) e^{-kh} + \frac{1}{2} \right) \right] \quad \dots (24)$$

where $S = a^2 \tau k =$ Value of Stokes Drift at the surface.

We note that (a)

$$\text{As buoy diameter } D \rightarrow 0, \quad \bar{V}_p \rightarrow \frac{a^2 \tau k e^{-kh}}{2} (1 + hk)$$

$$\text{and } \bar{V}_{cm} \rightarrow - \frac{a^2 \tau k}{2},$$

a result in agreement with equation 14, Appendix 1.

(b) As wavelength $\lambda \rightarrow \infty$. $k \rightarrow 0$,

$$\text{and } \overline{V_p - V_{cm}} \rightarrow S$$

(c) For $h \rightarrow 0$, $\overline{V_p - V_{cm}} \rightarrow S \cos \frac{kD}{2}$

The response has been plotted in Fig.6 for certain practical values of h/D and shows clearly the way in which the buoy acts as a low pass filter. The cut off frequency (taken as 70% of the surface Stokes Drift) is only slightly dependent on the current meter stem length h , for practical values of h . (Note that the response for $h = 0$ can only be described for small values of D/λ in this simple model: as D/λ approaches 1 the current meter spends part of the wave period out of water.)

The effect of this cut-off can only be assessed in relation to a specific wave spectrum. In Fig.7 we show the wave spectrum measured during Run 2 (p.10), and the computed spectrum of surface Stokes Drift associated with it. The contribution to the Drift of waves above 0.5Hz is negligible, and so the cut-off effect only begins to contribute at a buoy diameter of 1 - 2 metres.

DEFINITION LIST

a	-	wave amplitude	
σ	-	$2\pi/\text{wave period}$	
λ	-	wavelength	
k	-	$2\pi/\lambda$	
V_{cm}	-	current meter velocity)
)
)
V_p	-	water particle velocity)
)
)
V_b	-	buoy velocity)
)
x, y	-	horizontal axes	
z	-	vertical axis	
x_o	-	mean horizontal position of current meter	
z_o	-	mean depth of current meter below surface	
h	-	depth of current meter below streamline follower	
D	-	buoy diameter	
ϕ	-	waveslope at streamline follower	

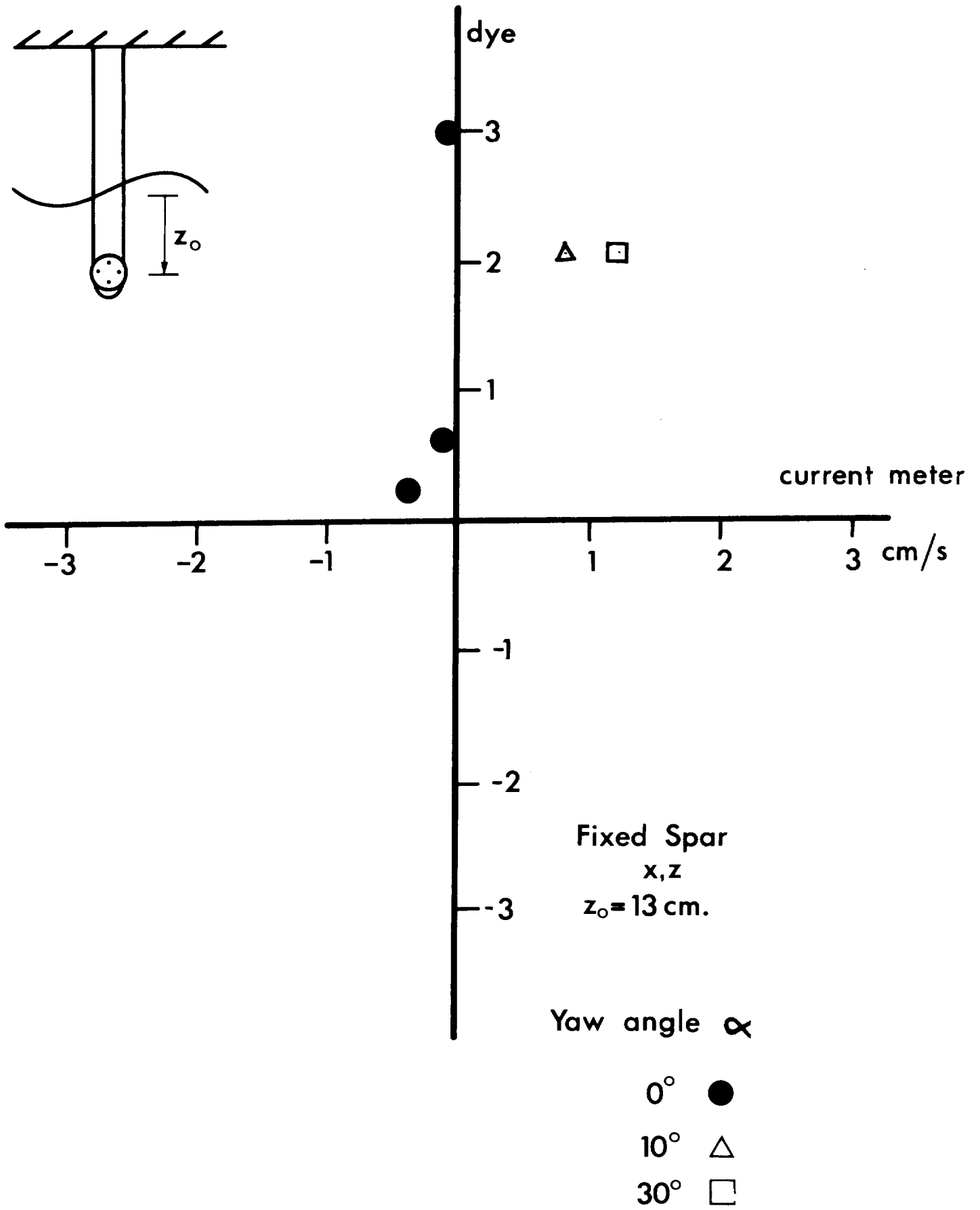


Fig. 1 (a)

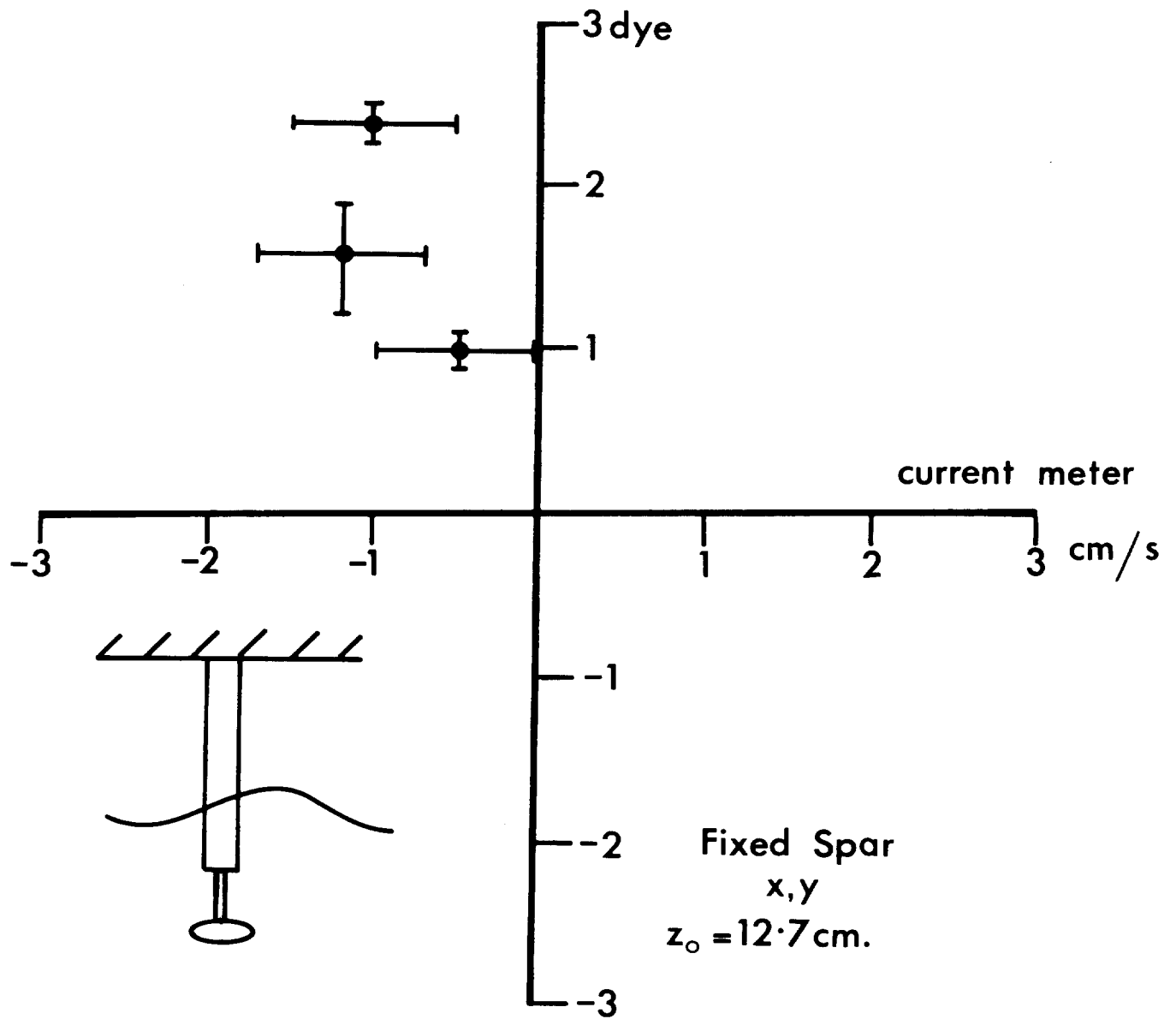


Fig. 1 (b)

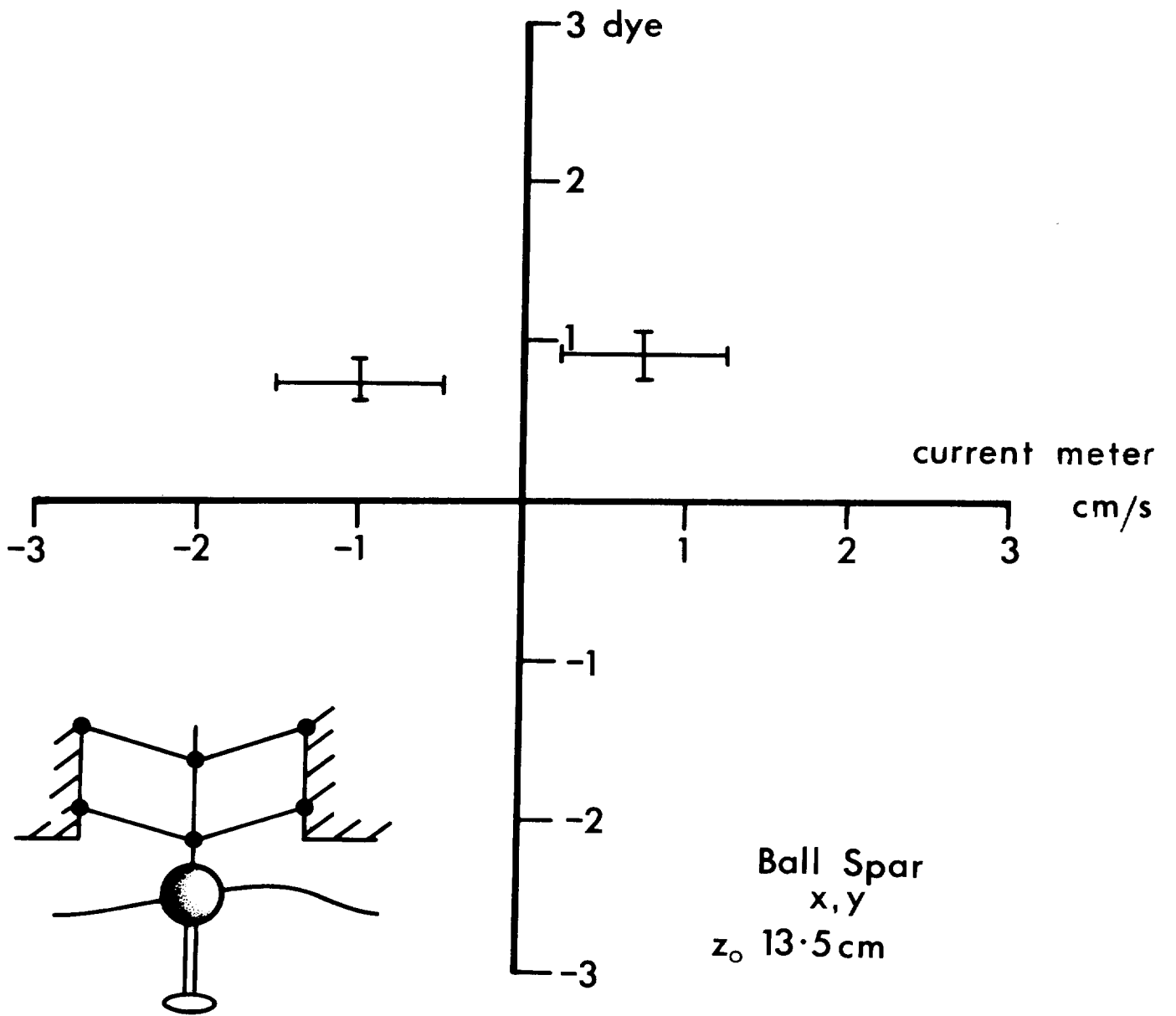


Fig. 1 (c)

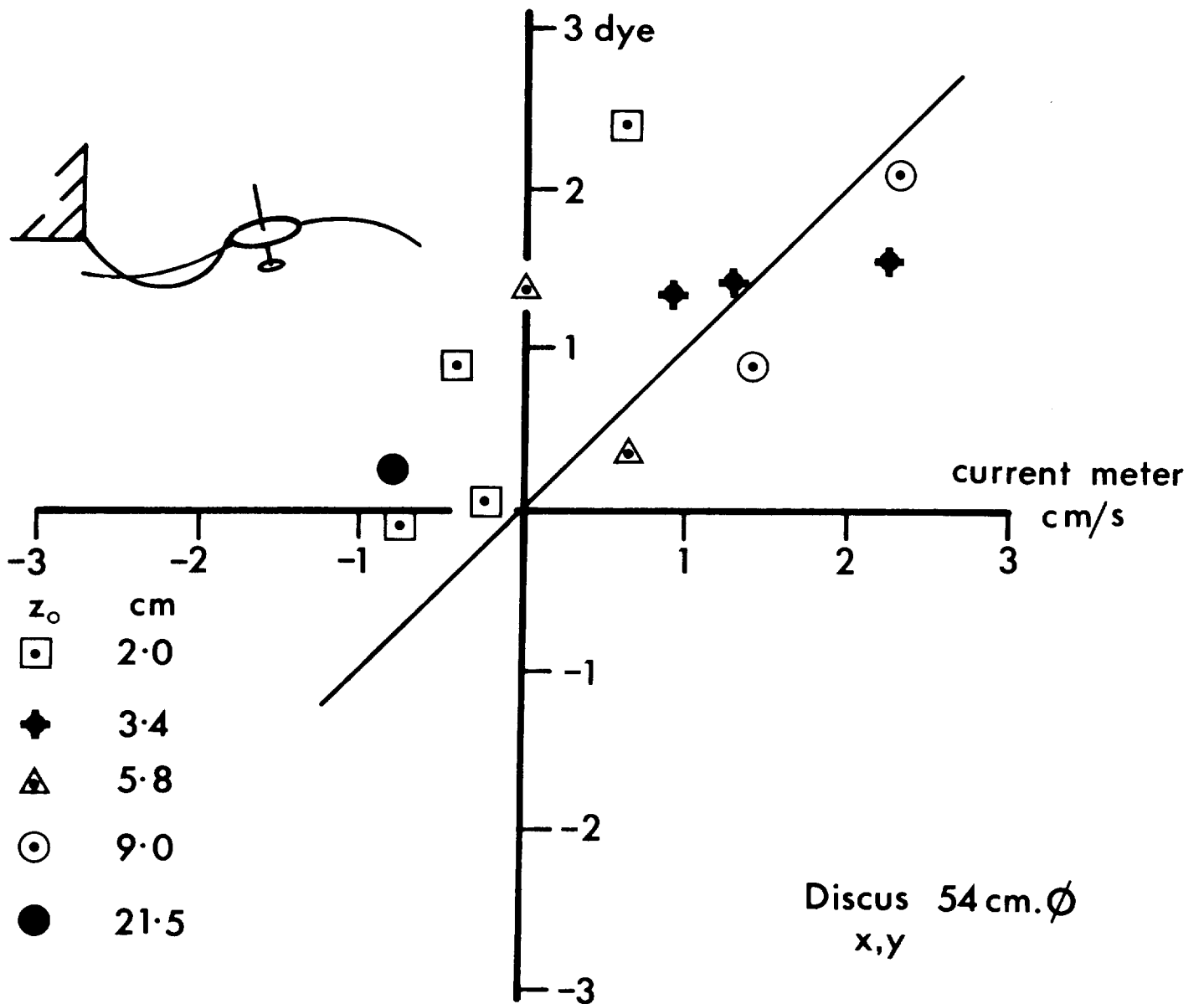


Fig. 1 (d)

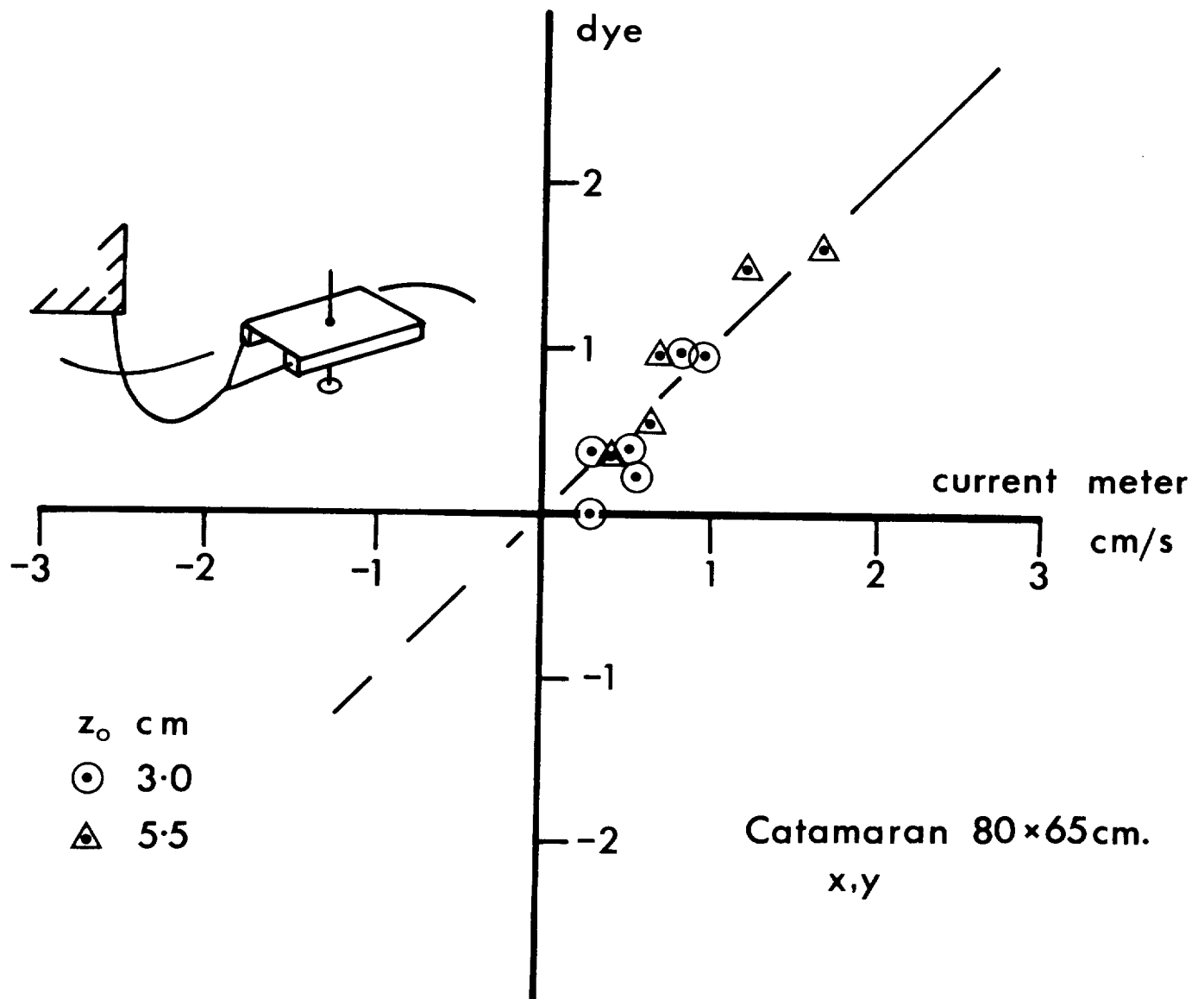


Fig. 1 (e)

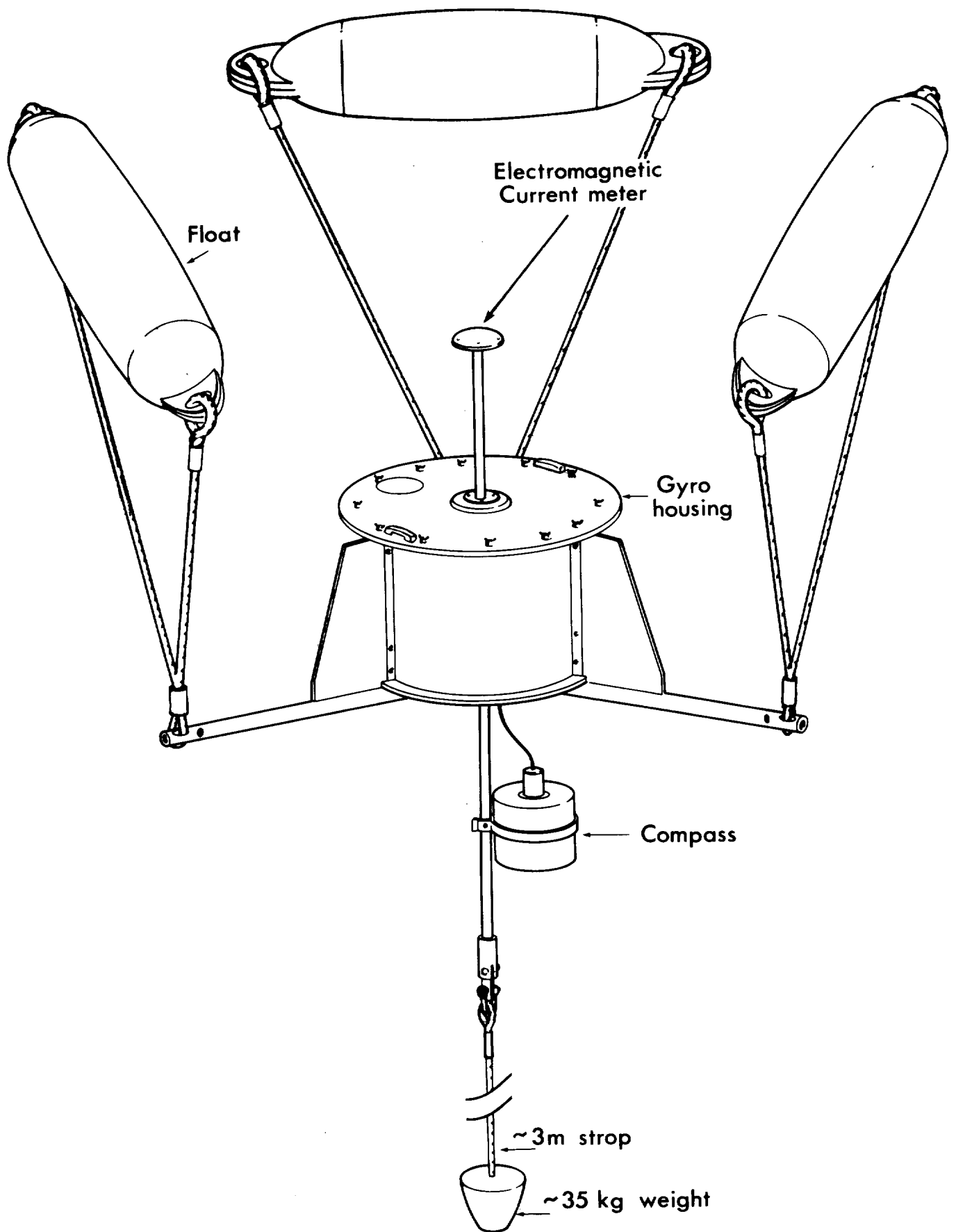


Fig.2 EM PR BUOY

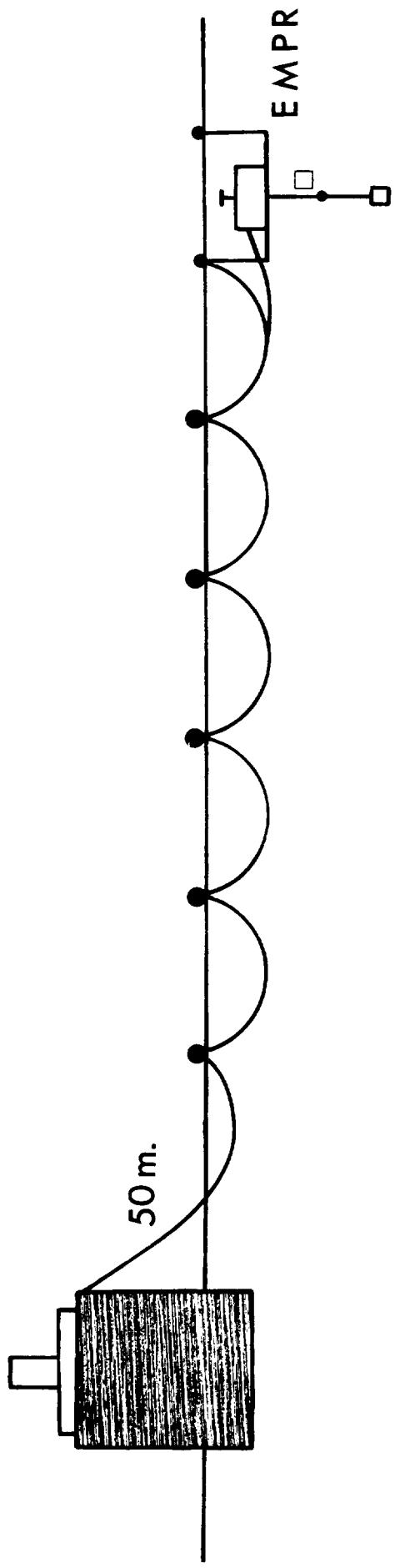


Fig. 3

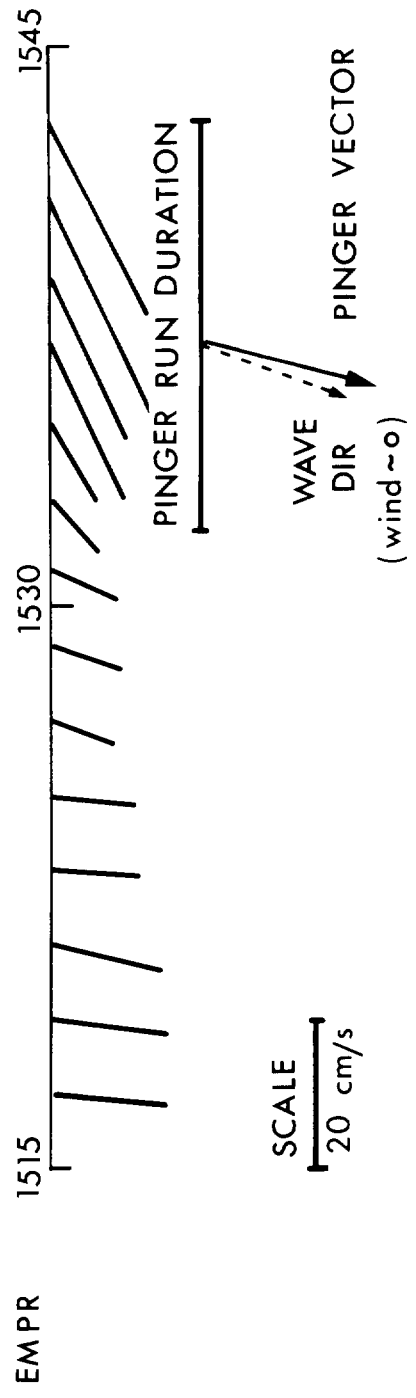
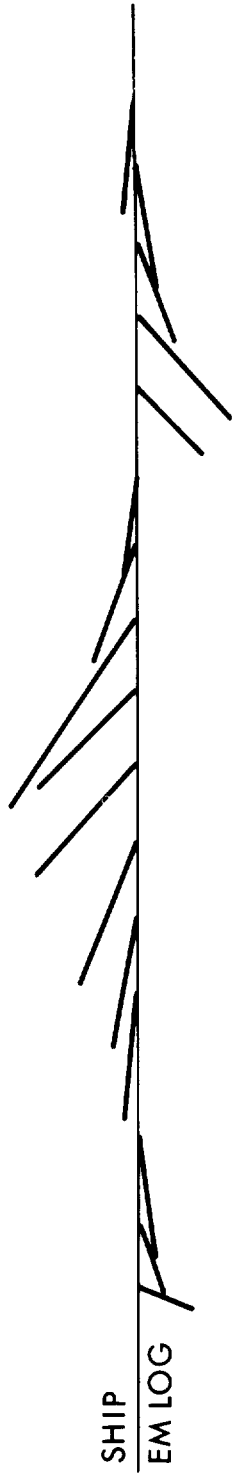


Fig. 4 (a) RUN 2

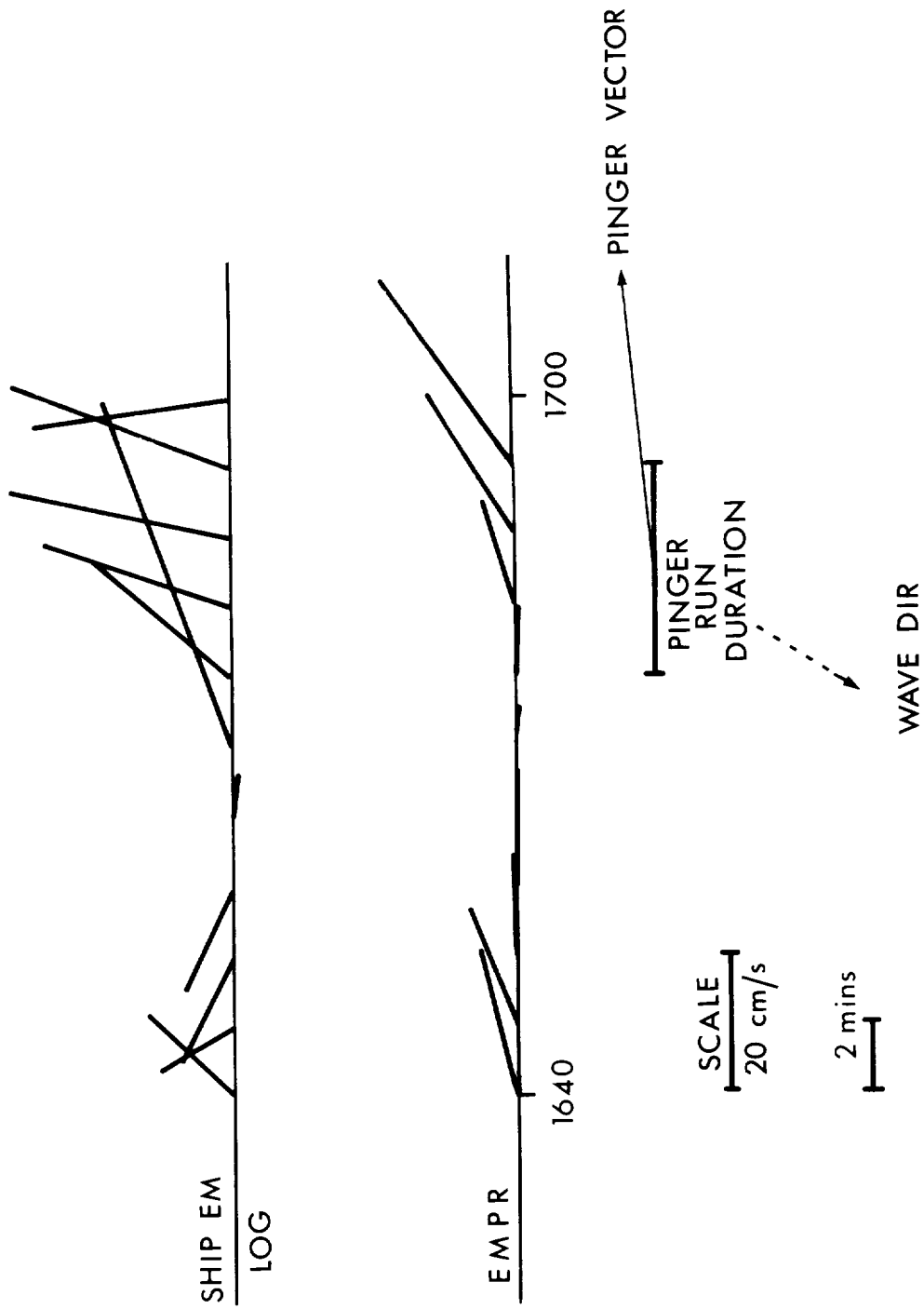


Fig. 4 (b) RUN 3

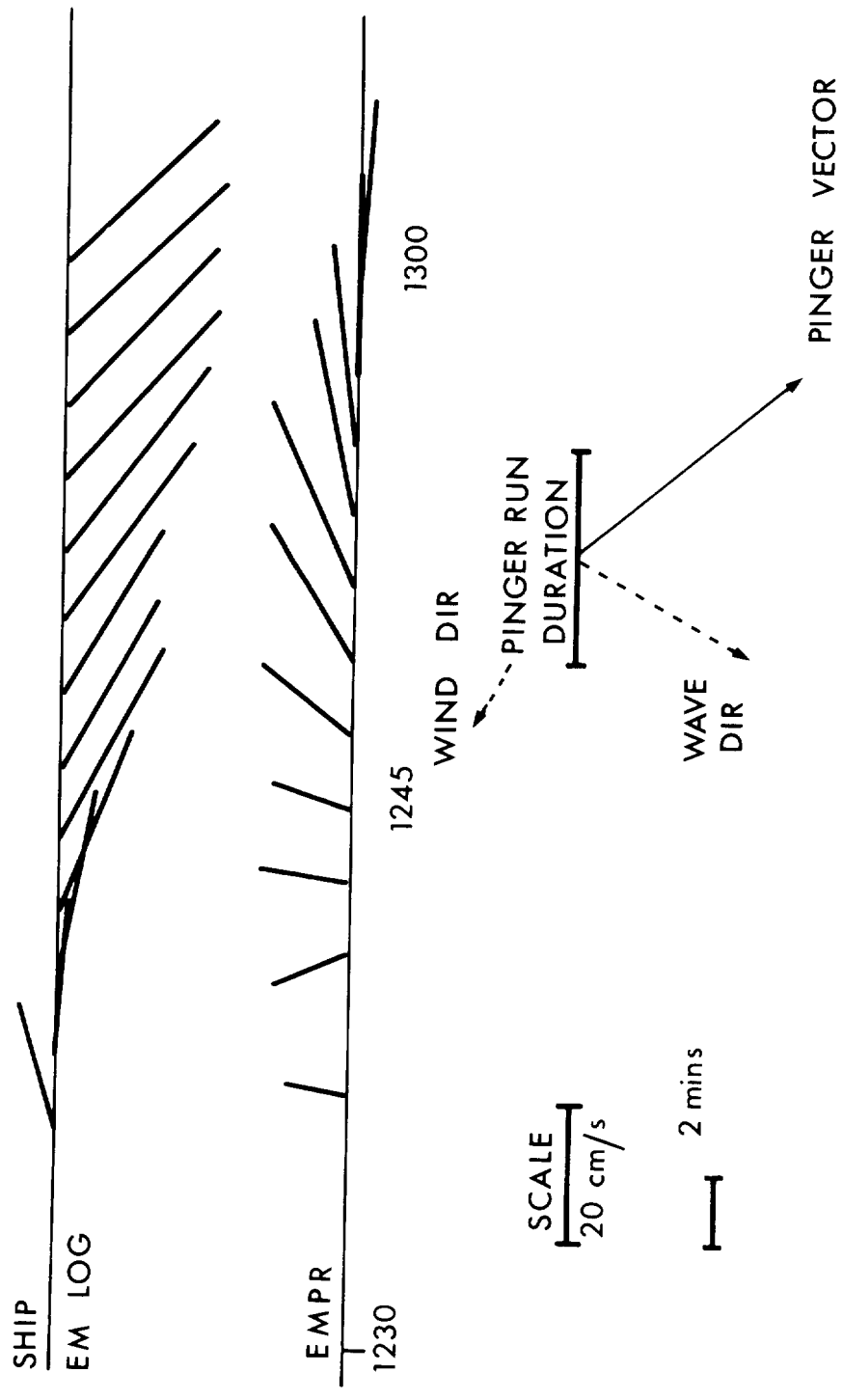
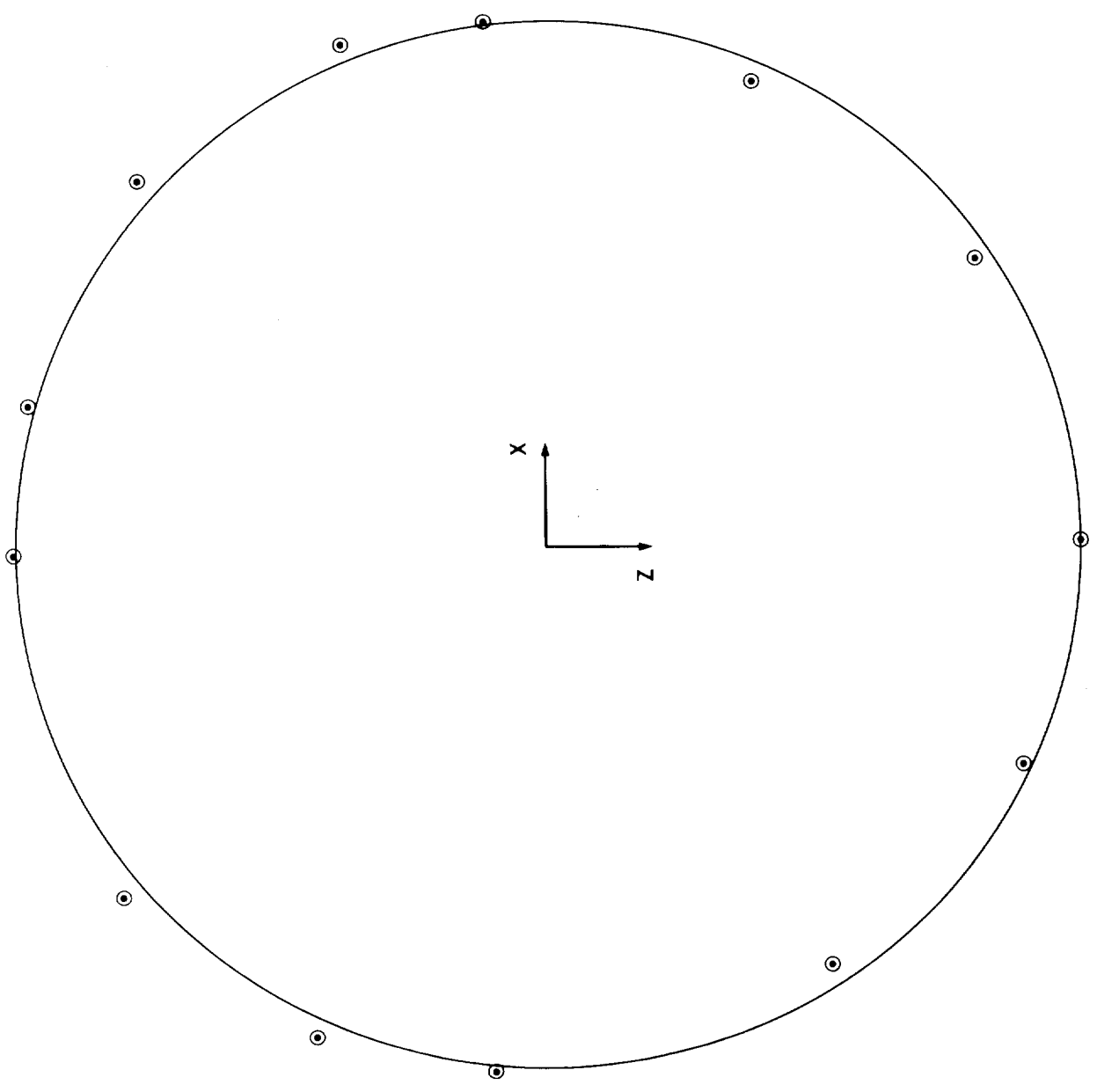


Fig. 4 (c) RUN 4

Fig.5

— CIRCULAR ORBIT $(\text{Displ})_z = f(t)$ only
⊙ ORBIT FOR $(\text{Displ})_z = f(t,x)$



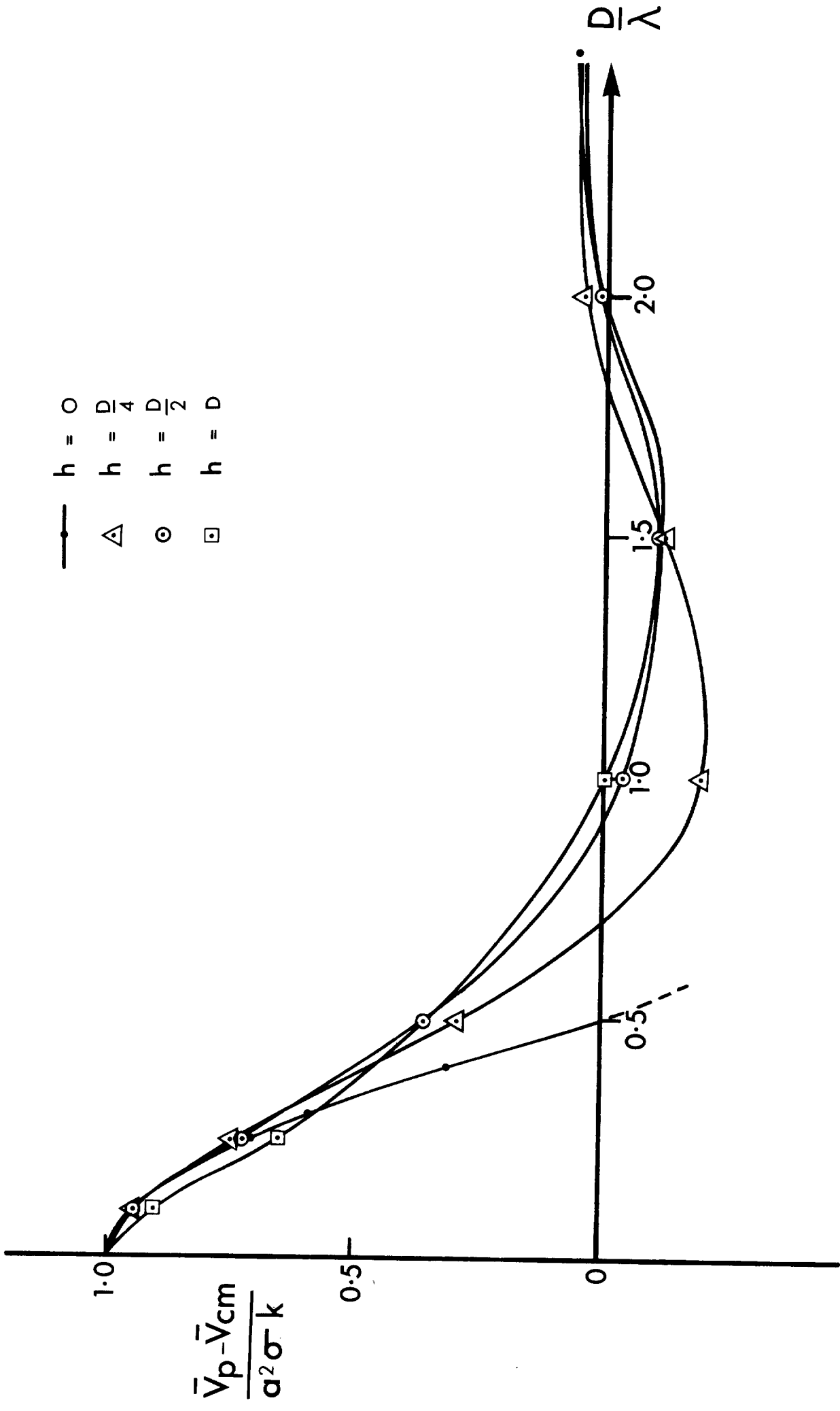


Fig. 6 Buoy/current meter response

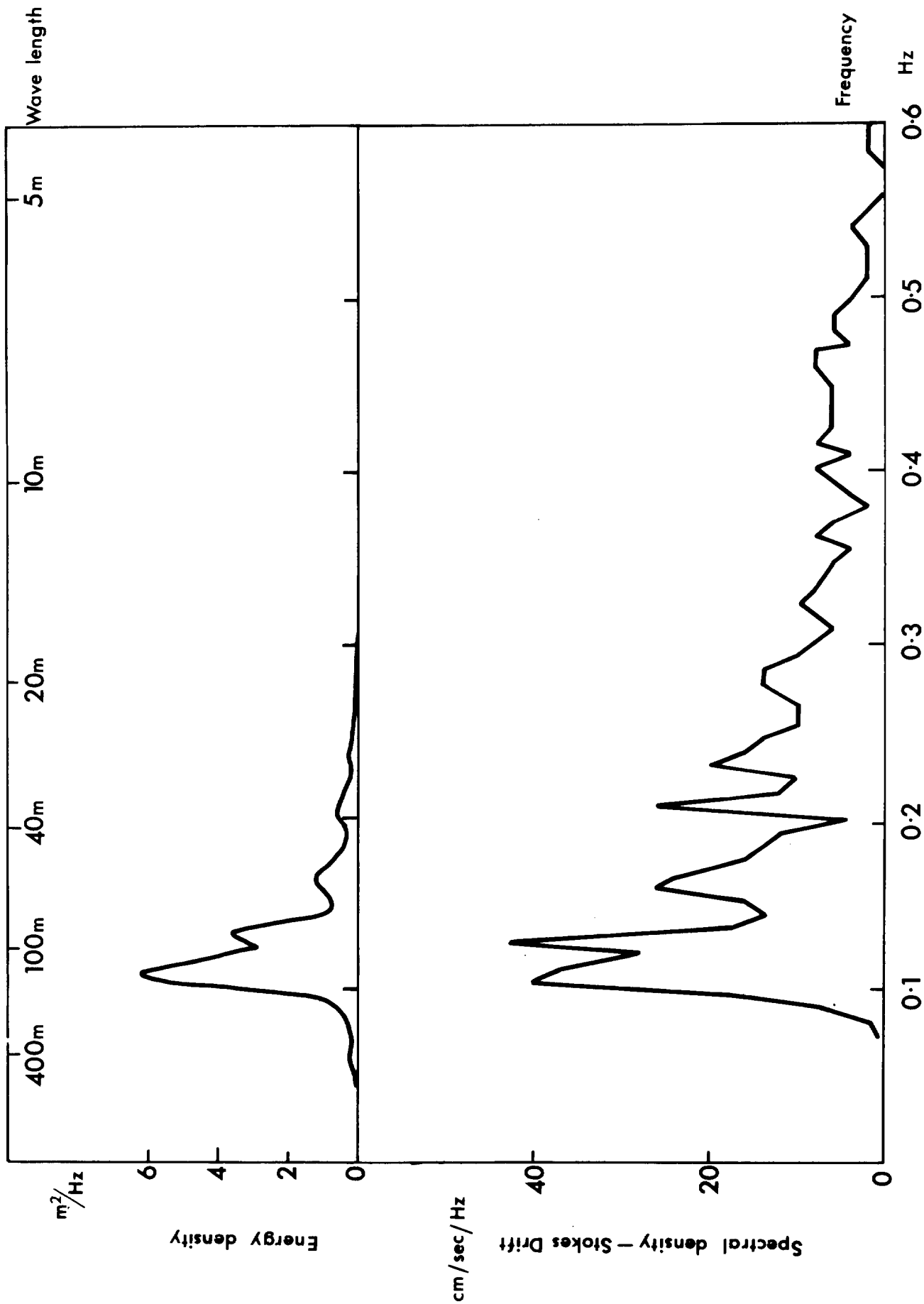


Fig. 7. Spectrum of wave energy and Stokes Drift (Surface), Run 2.